

Ecography

E6772

Fuller, M. M. and Enquist, B. J. 2011. Accounting for spatial autocorrelation in null models of tree species association. – *Ecography* 34: xxx–xxx.

Supplementary material

E6772

Fuller, M.M. and Enquist, B.J. 2011. Accounting for Spatial Autocorrelation in Null Models of Tree Species Association. — *Ecography* 000: 000000

Appendix 1: Details of Methodology

I: Scale Analysis of Patch Size

When a spatial pattern is autocorrelated, samples (e.g. species densities) recorded at nearby locations are not independent of each other, but show negative or positive correlation up to some distance. When other forms of nonstationarity also occur, such as changes in the sample variance with location, they can bias estimates of spatial autocorrelation (SAC). Nonstationarity refers to variation in the statistical moments of a pattern. For example, when a species mean density changes from one location to another, the mean is considered to be nonstationary. The mean and variance of the spatial patterns of many natural phenomena change with observation scale (Isaaks and Srivastava 1990). Therefore, it is advisable to recompute spatial statistics, using a range of observation scales, to compose a complete portrait of the pattern under investigation (Bellehumeur et al. 1997, Dungan et al. 2002).

For our study, we analyzed the influence of scale on the strength of SAC, and estimates of each species average patch size. To determine patch sizes, we followed Legendre and Legendre (1998; pp 721-724) and Fortin and Dale (2005; pp 127-131), who defined the patch size as the shortest distance at which the SAC in density equals zero (indicating no correlation between samples). Using the empirical stem map as a base map, we constructed a series of seven grid overlays. Each grid was assembled using a different, fixed grid cell length, ranging from 10 to 40m, in 5m increments. Our procedure is depicted as a flow chart in Fig. A1(a). For each overlay, we calculated the density (count/m²) of the stems in each grid cell, and then use these cell densities to compute the correlogram of Moran's *I*. By comparing the correlograms computed using different cell lengths, we determined the observation scale at which Moran's *I* had the highest values, indicating the observation scale at which the SAC of stem density was strongest. Using the same approach, we also determined whether increasing the observation scale substantially changed the estimates of patch size.

II: Scale Analysis of Relabelling

We performed a scale analysis of the array cells used for stem relabelling, to determine an appropriate cell length for constructing the SH models. To construct each SH model, we overlaid a grid (which we refer to as an array) of equal-sized cells onto the original stem map. The area covered by each array cell defines the boundaries of a local neighborhood of stems. Within each cell, we randomly exchanged the species labels among the individual stems, to generate a random pattern of nearest neighbor identities. The purpose of restricting relabelling to stems located only a short distance apart from each other is to preserve the observed SAC of each species. However, if the relabelling distance is too great, the procedure can potentially destroy, or significantly alter, a species' SAC. Therefore, to avoid significant changes to SAC, relabelling must be applied at a scale that is smaller than the minimum average patch size recorded for the species in the community.

To determine an appropriate scale for the relabelling procedure, we analyzed the effect of

relabelling distance on SAC. The procedure is depicted as a flow chart in Fig. A1(b). First, we determined the minimum patch radius shown by any species, as indicated by the correlograms. Next, we performed relabelling using a cell length equal to the minimum patch size. We then compared the observed correlograms before and after relabelling for changes in SAC. If the chosen cell length introduced significant changes in SAC, we reduced the cell length by 5m and repeated the above steps. We continued this procedure until we could no longer detect a significant change in SAC. We constructed the 999 SH models used for our analysis of the nearest-neighbor species-pair frequencies, using the cell length so determined.

References Cited in Appendix 1

- Bellehumeur, C., Legendre, P., and Marcotte, D. 1997. Variance and spatial scales in a tropical rain forest: changing the size of sampling units. — *Plant Ecol.* 130: 8998.
- Dungan, J.L., Perry, J.N., Dale, M.R.T., Legendre, P., Citron-Pousty, S., Fortin, M.-J., Jakomulska, A., Miriti, M. and Rosenberg, M.S. 2002. A balanced view of scale in spatial statistical analysis. — *Ecography* 25: 626-640.
- Fortin, M.-J. and Dale, M. 2005. *Spatial analysis a guide for ecologists*. — Cambridge Univ. Press.
- Isaaks, E.H. and Srivastava, R.M. 1990. *An Introduction to Applied Geostatistics*. — Oxford University Press.
- Legendre, P. and Legendre, L. 1998. *Numerical ecology*. Second English Ed. — Elsevier.

Appendix 2: Detailed Results

I: Observed Levels of Spatial Autocorrelation

We measured the SAC of the 51 species on the 14ha plot that were represented by 50 or more individuals. As a group, these 51 species represent 27 families, and account for 94.6% of the stems $> 3\text{cm}$ found on the plot. Figure A2 shows the correlograms of the 51 species, grouped by taxonomic family. The numbers in parentheses are the species' total abundance within the plot. The correlograms were computed for stem density samples, which were compiled by overlaying a grid (cell length = 20m) on the observed stem map (see main text: Methods, Measuring Spatial Autocorrelation: Correlograms). Because the spatial scale at which density is computed can influence the distance at which SAC is statistically significant, we analyzed the effect of scale on the correlograms in a separate procedure (Appendix 1, I).

II: Results of SAC Scale Analysis

Changing the observation scale (grid cell length) revealed that SAC was often strongest at scales $> 15\text{m}$. As examples of the effect of observation scale on SAC, Figure A3 shows the correlograms for the three most abundant species: *Astronium graveolens* (Jacq.), *Bursera simaruba* (Linn.), and *Exostema mexicanum* (Gray), representing four separate observation scales from 10 to 40m. As a group these three species account for 21% of the number of the stems and are represented in all parts of the study plot. For grid cell lengths $\leq 25\text{m}$, the correlograms of these species were similar in character, and revealed little dependence of patch size on observation scale. When larger grid cells were used, the number of significant distance classes declined, with most of the species showing non-significant SAC at distances greater than $\approx 25\text{m}$. The average patch radius for *A. graveolens*, *B. simaruba*, and *E. mexicanum*, was ≈ 70 , 80, and 100m respectively.

Changing the grid cell length from 10 to 20m caused the patch size estimates for some species to shift to the right, indicating that these scales were too small to accurately portray the empirical patterns. For cell lengths of 20m, the estimates of patch radius stabilized, and revealed a minimum radius of 40m for the 51 species examined. The patch size distribution indicated that labelling at distances $< 50\text{m}$ would incorporate the observed pattern of local aggregation for most species. However, our analysis of relabelling effects (Appendix 1, II) revealed that using a relabelling distance $\geq 25\text{m}$ led to significant differences in SAC between the observed and modelled communities. Reducing the array cell length from 40m to 25m mitigated the effects of labelling on SAC. Therefore, we constructed the HP models using a 25m array cell length (625m^2 cell area).

Appendix 3: Species Tables

Table A1. Species List

Numeric code and plot abundance for each species recorded within the study plot.

Family	Species	Code	Abundance
Anacardiaceae	<i>Astronium graveolens</i>	36	1078
Anacardiaceae	<i>Spondias mombin</i>	57	203
Anacardiaceae	<i>Spondias purpurea</i>	21	67
Annonaceae	<i>Annona purpurea</i>	27	118
Annonaceae	<i>Annona reticulata</i>	38	54
Annonaceae	<i>Sapranthus palanga</i>	90	386
Apocynaceae	<i>Plumeria rubra</i>	189	3
Apocynaceae	<i>Stemmadenia obovata</i>	68	326
Apocynaceae	<i>Thevetia ovata</i>	210	1
Araliaceae	<i>Sciadodendron excelsum</i>	108	24
Asteraceae	<i>Critonia sexangulare</i>	965	3
Bignoniaceae	<i>Crescentia alata</i>	155	1
Bignoniaceae	<i>Godmania aesculifolia</i>	111	19
Bignoniaceae	<i>Tabebuia impetiginosa</i>	975	1
Bignoniaceae	<i>Tabebuia ochracea</i>	33	477
Bignoniaceae	<i>Tabebuia rosea</i>	74	22
Bombacaceae	<i>Bombacopsis quinatum</i>	56	45
Bombacaceae	<i>Pseudobombax septinatum</i>	192	8
Boraginaceae	<i>Cordia alliodora</i>	62	93
Boraginaceae	<i>Cordia panamensis</i>	18	271
Burseraceae	<i>Bursera simaruba</i>	23	1004
Burseraceae	<i>Bursera tomentosa</i>	143	2
Caesalpinaceae	<i>Bauhinia unguolata</i>	46	90
Caesalpinaceae	<i>Hymenaea courbaril</i>	171	4
Caesalpinaceae	<i>Senna atromaria</i>	420	12
Caesalpinaceae	<i>Swartzia cubensis</i>	205	100

Table A1. Species List (continued)

Family	Species	Code	Abundance
Capparidaceae	<i>Capparis frondosa</i>	316	6
Capparidaceae	<i>Capparis indica</i>	76	373
Chrysobalanaceae	<i>Licania arborea</i>	30	97
Cochlospermaceae	<i>Cochlospermum vitifolium</i>	9	160
Ebenaceae	<i>Diospyros nicaraguensis</i>	159	47
Euphorbiaceae	<i>Adelia triloba</i>	946	30
Euphorbiaceae	<i>Margaritaria nobilis</i>	133	10
Euphorbiaceae	<i>Sapium thelocarpum</i>	41	103
Euphorbiaceae	<i>Sebastiania pavoniana</i>	169	236
Fabaceae	<i>Andira inermis</i>	64	2
Fabaceae	<i>Ateleia herbert-smithii</i>	110	240
Fabaceae	<i>Dalbergia retusa</i>	158	9
Fabaceae	<i>Diphysa robinoides</i>	160	7
Fabaceae	<i>Gliricidia sepium</i>	166	1
Fabaceae	<i>Lonchocarpus acuminatus</i>	65	481
Fabaceae	<i>Lonchocarpus costaricensis</i>	85	86
Fabaceae	<i>Lonchocarpus oliganthus</i>	967	2
Fabaceae	<i>Lonchocarpus parviflorus</i>	10	549
Fabaceae	<i>Lonchocarpus</i> spp.	258	1
Fabaceae	<i>Machaerium biovulatum</i>	53	176
Fabaceae	<i>Myrospermum frutescens</i>	99	54
Fabaceae	<i>Pterocarpus rohrii</i>	981	2
Flacourtiaceae	<i>Casearia arguta</i>	11	57
Flacourtiaceae	<i>Xylosoma flexuosa</i>	217	5
Flacourtiaceae	<i>Zuelania guidonia</i>	220	31
Lauraceae	<i>Ocotea veraguensis</i>	1	325
Malpighiaceae	<i>Bunchosia biocellata</i>	142	158
Malpighiaceae	<i>Byrsonima crassifolia</i>	144	4

Table A1. Species List (continued)

Family	Species	Code	Abundance
Melastomataceae	<i>Miconia argentea</i>	179	4
Meliaceae	<i>Cedrela odorata</i>	80	55
Meliaceae	<i>Guarea excelsa</i>	88	25
Meliaceae	<i>Swietenia humilis</i>	207	32
Meliaceae	<i>Swietenia macrophylla</i>	206	16
Meliaceae	<i>Trichilia americana</i>	14	55
Meliaceae	<i>Trichilia cuneata</i>	12	150
Meliaceae	<i>Trichilia hirta</i>	13	208
Meliaceae	<i>Trichilia trifolia</i>	211	17
Mimosaceae	<i>Albizzia adinocephala</i>	44	71
Mimosaceae	<i>Enterolobium cyclocarpum</i>	16	13
Mimosaceae	<i>Inga vera</i>	89	4
Mimosaceae	<i>Lysiloma seemannii</i>	176	37
Mimosaceae	<i>Pithecellobium saman</i>	48	11
Moraceae	<i>Brosimum alicastrum</i>	141	16
Moraceae	<i>Castilla elastica</i>	149	4
Moraceae	<i>Cecropia peltata</i>	131	18
Moraceae	<i>Ficus ovalis</i>	24	4
Moraceae	<i>Ficus</i> spp.	164	6
Moraceae	<i>Maclura tinctoria</i>	2	194
Moraceae	<i>Trophis racemosa</i>	31	18
Myrtaceae	<i>Eugenia salamensis</i>	98	24
Olacaceae	<i>Schoepfia schreberi</i>	101	60
Opiliaceae	<i>Agonandra macrocarpa</i>	325	33
Proteaceae	<i>Roupala montana</i>	198	15
Rhamnaceae	<i>Karwinskia calderoni</i>	173	23
Rhamnaceae	<i>Krugiodendron ferreum</i>	934	1
Rhamnaceae	<i>Zizyphus guatemalensis</i>	720	1

Table A1. Species List (continued)

Family	Species	Code	Abundance
Rubiaceae	<i>Calycophyllum candidissimum</i>	7	508
Rubiaceae	<i>Chomelia spinosa</i>	19	466
Rubiaceae	<i>Couterea hexandra</i>	939	3
Rubiaceae	<i>Exostema mexicanum</i>	75	709
Rubiaceae	<i>Genipa americana</i>	165	149
Rubiaceae	<i>Guettarda macrosperma</i>	79	347
Rubiaceae	<i>Randia karstenii</i>	52	69
Rubiaceae	<i>Randia subcordata</i>	8	633
Rutaceae	<i>Xanthoxylum setulosum</i>	60	51
Sapindaceae	<i>Cupania guatemalensis</i>	5	66
Sapindaceae	<i>Dipterodendron costaricensis</i>	118	38
Sapindaceae	<i>Thouinidium decandrum</i>	59	44
Sapotaceae	<i>Chrysophyllum brenesii</i>	935	23
Sapotaceae	<i>Manilkara chicle</i>	78	222
Sapotaceae	<i>Mastichodendron capiri</i>	100	69
Simaroubaceae	<i>Simarouba glauca</i>	67	75
Solanaceae	<i>Cestrum</i> sp.	260	1
Sterculiaceae	<i>Guazuma ulmifolia</i>	22	400
Sterculiaceae	<i>Sterculia apetala</i>	719	2
Tiliaceae	<i>Luehea candida</i>	58	2
Tiliaceae	<i>Luehea speciosa</i>	112	560
Tiliaceae	<i>Luehea</i> spp.	233	244
Verbenaceae	<i>Rhederia trinervis</i>	195	176

Table A2. Most Frequent Species Pairs

Table A2 shows the species that occurred as nearest-neighbors with the highest observed frequency, including conspecific pairs (top 50, ranked by number of pair-wise occurrences). Rank = frequency rank of species pair; Sp1, Sp2 = numeric code for each species (see Table A1 for species names); Frequency = number of pair-wise occurrences as nearest neighbors within the study plot.

Rank	Sp1	Sp2	Frequency
1	10	10	183
2	36	36	174
3	23	23	145
4	8	8	103
5	36	23	100
6	65	65	92
7	7	7	89
8	75	36	81
9	75	75	67
10	23	36	65
11	36	75	63
12	19	8	60
13	23	7	60
14	36	8	59
15	23	8	58
16	36	7	55
17	75	7	54
18	75	8	54
19	169	169	50
20	75	23	50
21	8	36	50
22	1	1	47
23	112	8	47
24	8	19	47
25	23	22	46
26	65	8	46
27	7	23	46

Table A2. Most Frequent Species Pairs (continued)

No.	Sp1	Sp2	Frequency
28	112	36	44
29	112	23	43
30	33	10	43
31	8	23	43
32	169	36	42
33	22	23	42
34	65	23	41
35	23	10	40
36	110	110	39
37	22	22	39
38	33	23	39
39	10	23	38
40	19	23	38
41	8	7	38
42	33	36	37
43	36	10	37
44	7	36	37
45	112	7	36
46	36	1	36
47	36	2	36
48	23	19	35
49	19	19	34
50	112	112	33

Scale Analysis Algorithms

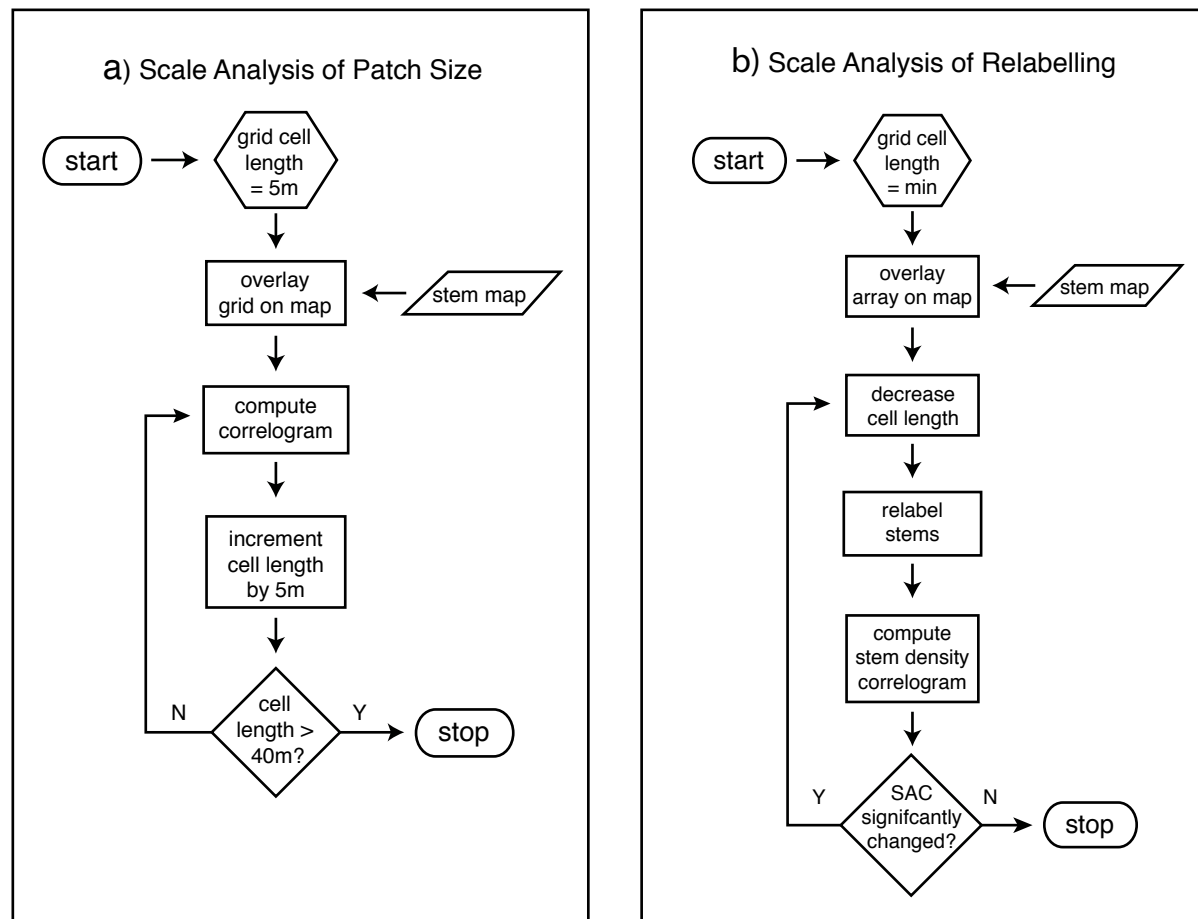


Figure A1: Flow charts depicting the steps used for (a) the scale analysis of patch size (effect of observation scale on SAC), and (b) the scale analysis of relabelling (effect of relabelling scale on SAC). See Appendix 1 text for details.

Species Correlograms

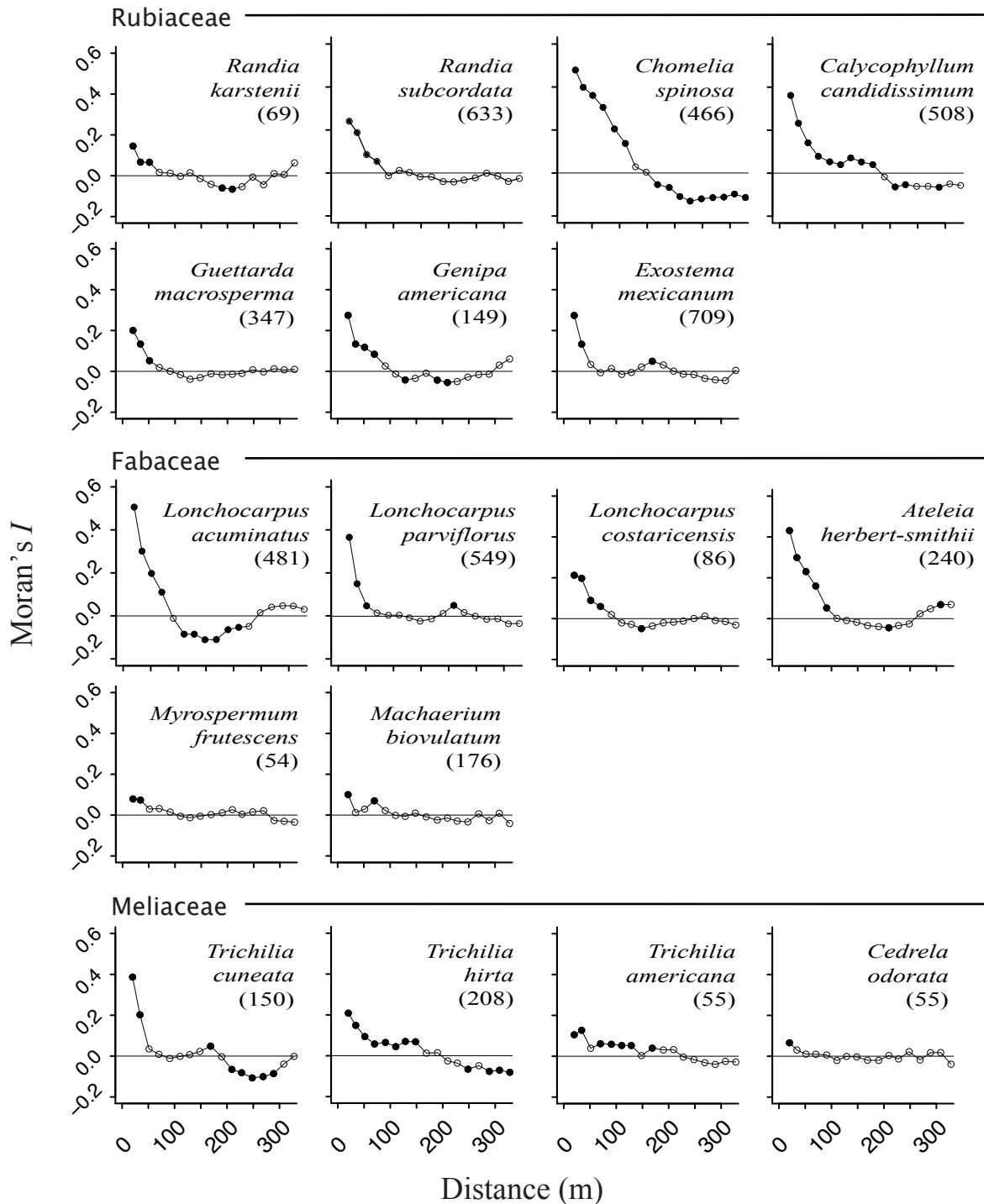
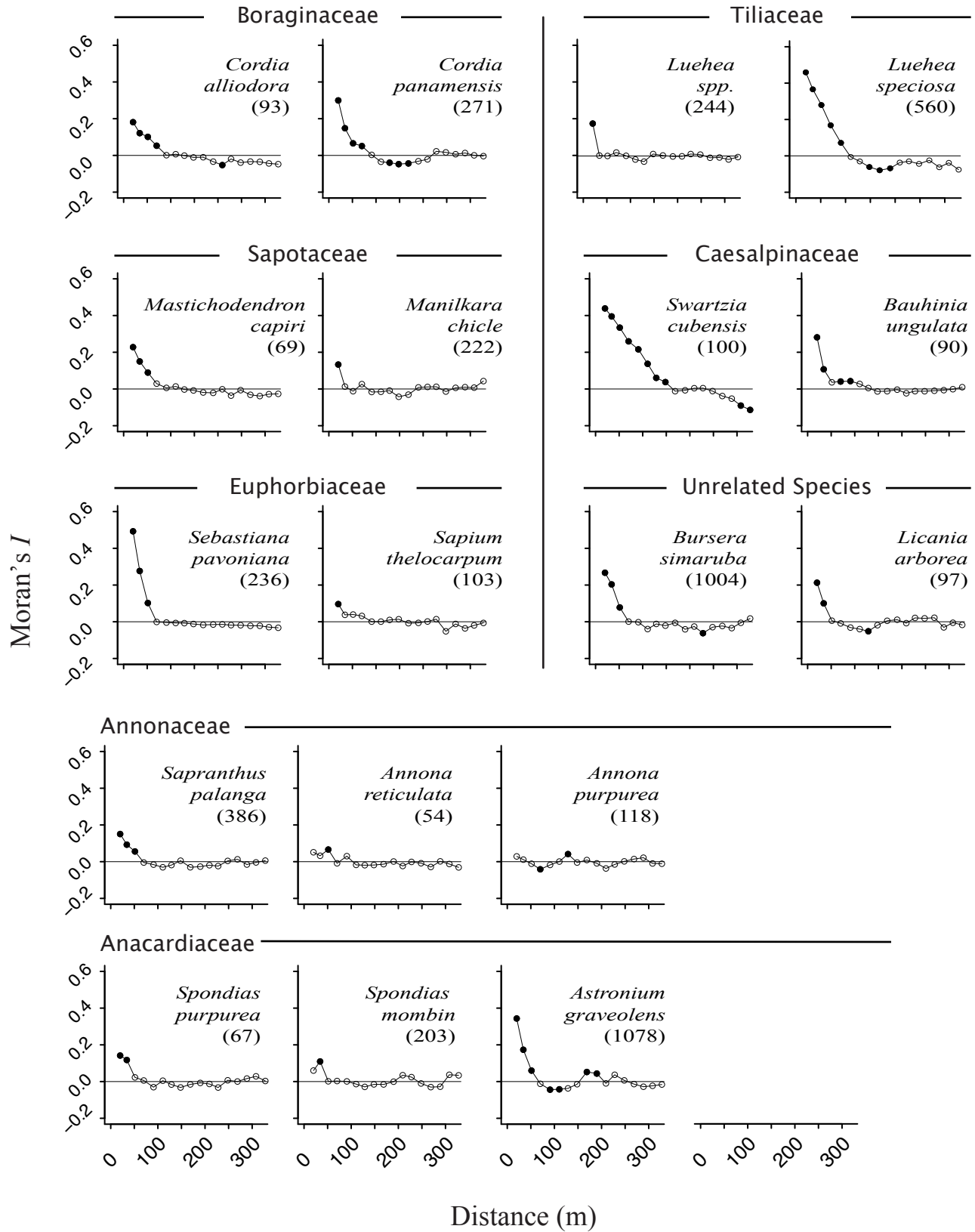
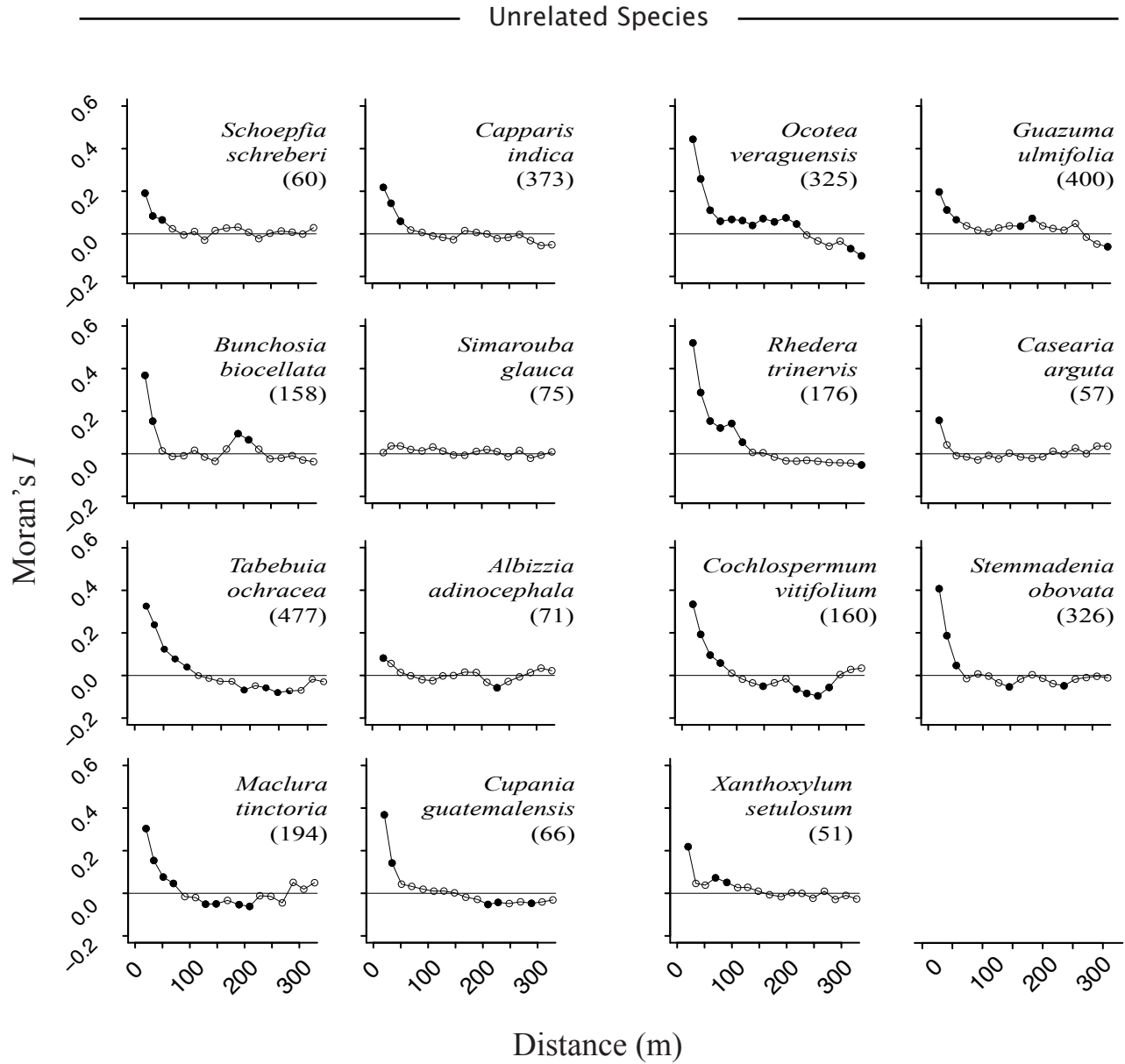


Figure A2: Correlograms of Moran's I for the 51 species with at least 50 individual stems on the plot. Where two or more members of the same taxonomic family were represented, we grouped them together by Family name. Otherwise, species are grouped under the heading "Unrelated Species" (family names shown in Table A1). Solid horizontal line = zero correlation. Open circles = values not significant based upon 999 permutations. Closed circles = significant values ($p = 0.05$). Values in parentheses correspond to the species' plot abundance.





Scale Analysis of Spatial Autocorrelation

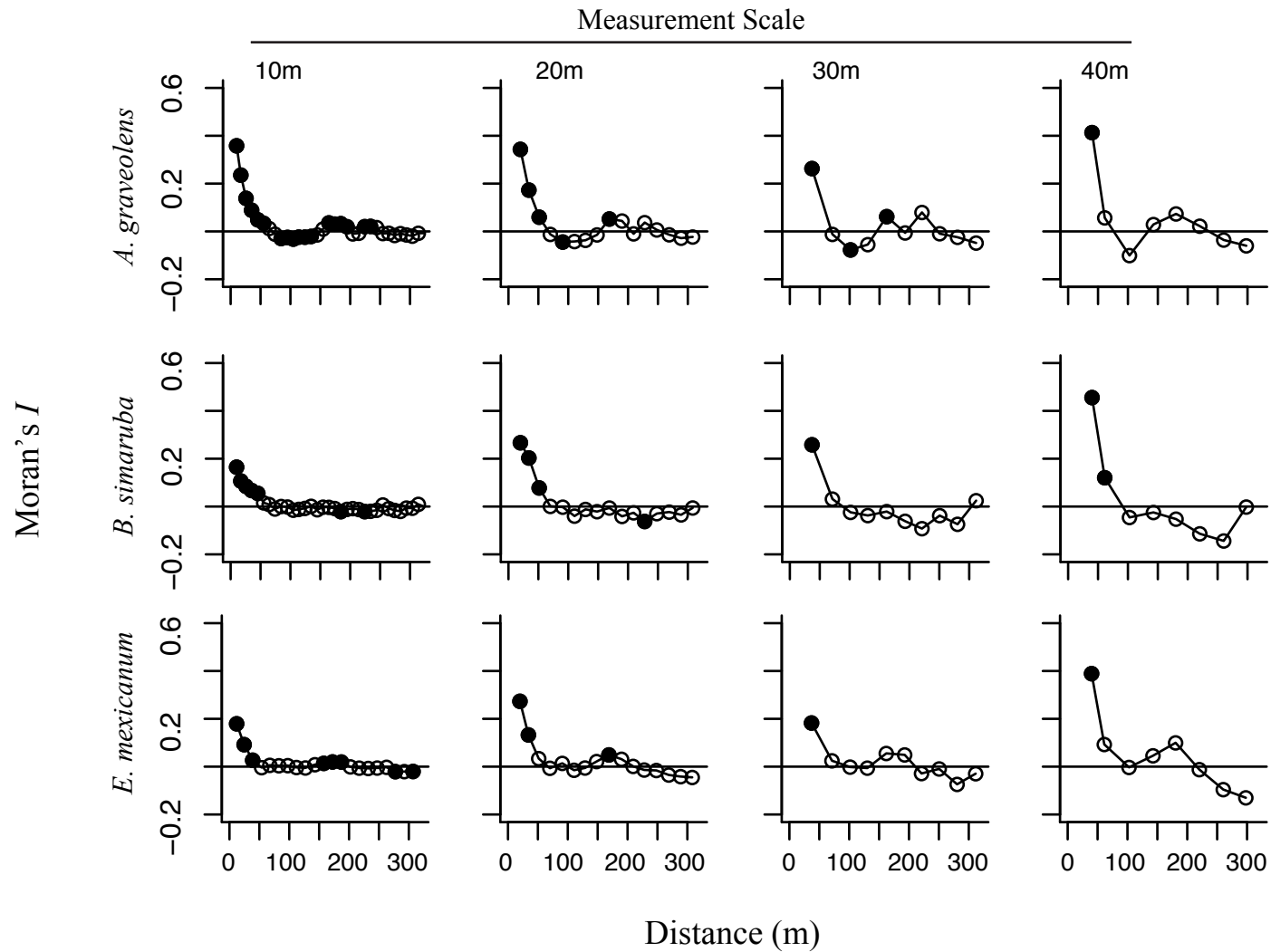


Figure A3. The figure shows the effect of observation (measurement) scale on correlograms of Moran's I in stem density, for the three most common species on the plot. Symbols as in Fig. A2. Values above each column (Measurement Scale) indicate length of array cells used to compute stem density.